



Mechanisms and variances of rotation-induced brain injury: a parametric investigation between head kinematics and brain strain

Kewei Bian¹ · Haojie Mao^{1,2}

Received: 23 March 2019 / Accepted: 12 May 2020 / Published online: 24 May 2020
© Springer-Verlag GmbH Germany, part of Springer Nature 2020

Abstract

There lacks a comprehensive understanding of the correlation between head kinematics and brain strain especially deep-brain strain, partially resulting the deficiency of understanding brain injury mechanisms and the difficulty of choosing appropriate brain injury metrics. Hence, we simulated 76 impacts that were focused on concussion-relevant rotational kinematics and evaluated cumulative strain damage measure (CSDM) and average strain that could represent brain strain distribution. For the whole brain, axial rotation induced the highest CSDM, while lateral bending produced the lowest CSDM. However, for the deep-brain components, lateral bending produced the highest CSDM to the corpus callosum and thalamus. We further confirmed that brain strain was mainly produced by rotational kinematics, for which the effect of rotational deceleration could not be ignored with the deceleration influencing CSDM20 up to 27%. Our data supported that peak rotational velocity correlated to brain strain with an average R^2 of 0.77 across various impact directions and different shapes of loading curves. The correlation between peak rotational velocity and brain strain reached to an average R^2 of 0.99 for each specific impact direction. Our results supported using direction-specific peak rotation velocity for predicting strain-related brain injury. Additionally, we highlighted the importance of investigating whole-brain and deep-brain strain, as well as considering rotational deceleration.

Keywords Concussion · Injury mechanism · Impact direction · Rotational velocity · Injury metric

1 Introduction

There are 1.6–3.8 million sports-related Traumatic Brain Injuries (TBIs) including concussions in USA alone (Langlois et al. 2006). Concussion induces symptoms such as memory loss, cognitive deficits, and balance disturbances (Guskiewicz et al. 2007; McCrory et al. 2009). Nowadays, concussion is widely investigated using clinical, pathological, and biomechanical methods (Guskiewicz and Mihalik 2011; McCrory et al. 2009). For biomechanical methods, both experimental methods and finite element (FE) models are extensively used to explore the tissue-level responses

of the brain due to impacts (Kleiven 2007; Post et al. 2012; Sanchez et al. 2018).

Concussion has been demonstrated to be related to linear and rotational head kinematics. Pellman et al. reported that concussive players experienced peak linear acceleration of 98 ± 28 g (Pellman et al. 2003b). The peak linear acceleration ranged from 61 to 144 g (Zhang et al. 2004). Margulies and Thibault suggested the threshold of 1600 rad/s^2 based on the primate model (Margulies and Thibault 1992). Rowson et al. (2012) published the thresholds of concussion as 5260, 5281, 6383, 6945 and 7483 rad/s^2 for the concussion risk of 10%, 25%, 50%, 75% and 90%, respectively. Most concussive cases happen with the peak rotational acceleration around 5 krad/s^2 (Fig. 1a) (Beckwith et al. 2013; Guskiewicz and Mihalik 2011; Hoshizaki et al. 2017; Pellman et al. 2003a, 2003b; Rowson et al. 2012). For impact durations, Greenwald et al. reported that 95% of impacts happened between 5.5 and 13.7 ms (Greenwald et al. 2008). Rowson et al. (2009) recorded the average duration of 14 ms for helmeted head impacts. Based on the above data, systematically

✉ Haojie Mao
hmao8@uwo.ca

¹ Department of Mechanical and Materials Engineering, Faculty of Engineering, Western University, London, ON N6A 5B9, Canada

² School of Biomedical Engineering, Western University, London, ON N6A 5B9, Canada

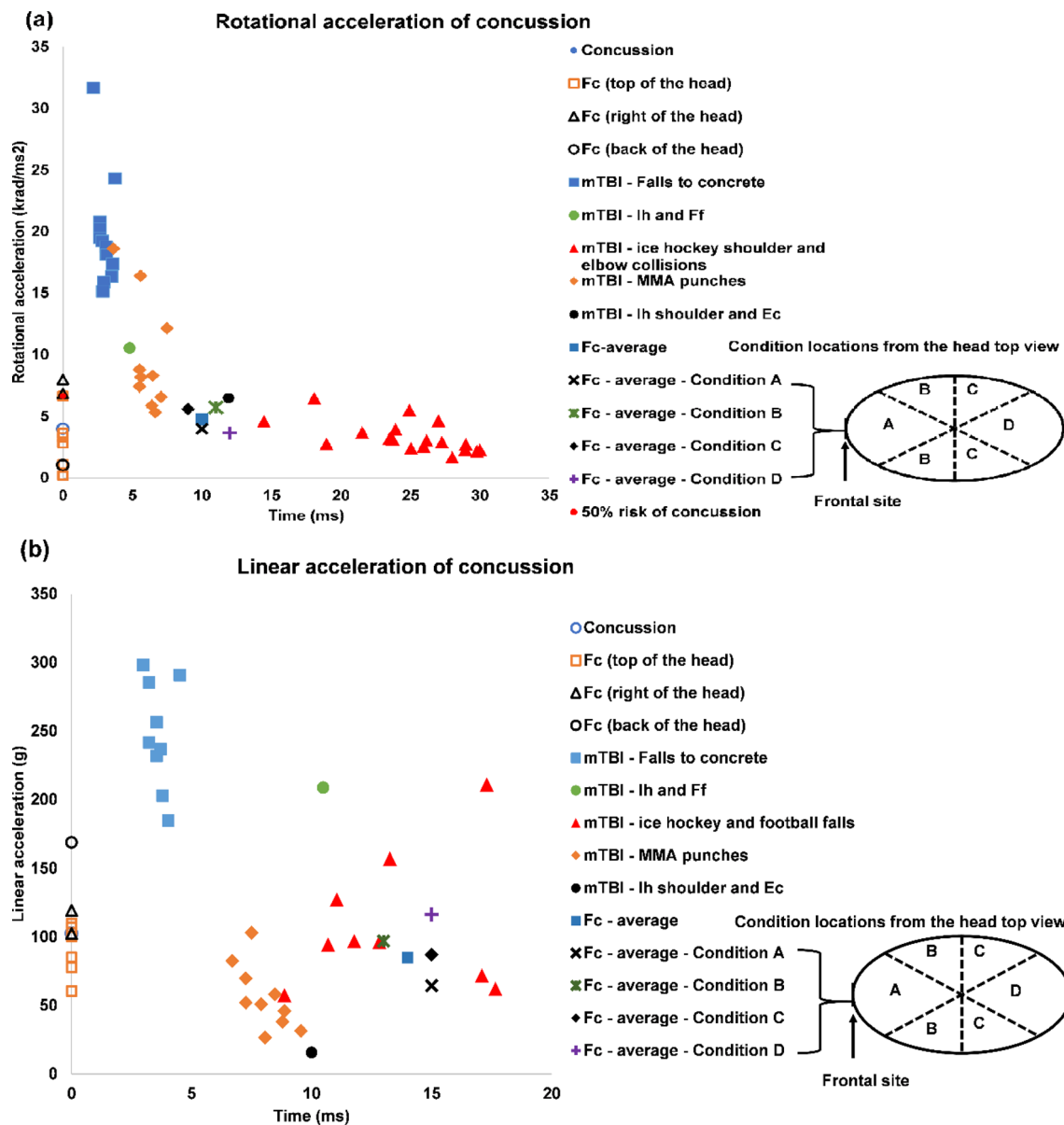


Fig. 1 Rotational and linear accelerations that cause concussion. **a** Literature-reported rotational acceleration of concussion; **b** Literature-reported linear acceleration of concussion (Beckwith et al. 2013; Guskiewicz and Mihalik 2011; Hoshizaki et al. 2017; Pellman et al.

2003a; Pellman et al. 2003b; Rowson et al. 2012; Viano and Pellman 2005). Data with unknown duration are shown on the vertical axis. *Fc* football concussion, *lh* ice hockey, *Ff* football fall, *Ec* elbow collision, *mTBI* mild traumatic brain injury, *MMA* mixed martial art

investigating brain responses induced by reported head kinematics related to concussion will be critical.

The brain response is crucial for predicting TBI including concussion. Kleiven summarized 10 predictors that were widely used for predicting TBI. The predictors relevant to brain responses include strain, strain rate, product of strain and strain rate, cumulative strain damage measure (CSDM), strain energy density, maximum pressure, magnitude of minimum pressure and von Mises effective stress (Kleiven 2007). The use of maximum principal strain (MPS) was suggested by Bain and Meaney (2000) and Thibault

et al. (1990). Von Mises stresses and strain energy were used as the predictors by Shreiber et al. (1997). The product of strain and strain rate was suggested by Viano and Lovsund (1999) and King et al. (2003). The CSDM was suggested as the predictor of brain responses by Kimpara and Iwamoto (2012); Takhounts et al. (2013, 2003, 2008).

Brain strains are of significance in predicting TBI or concussion. There were studies reporting the range of 0.19–0.21 for mild TBI (Kleiven 2007; Zhang et al. 2004) based on the whole-brain strains. However, it's accepted that deformation produced by impact can cause different symptoms in various

brain regions (Post et al. 2014), highlighting the importance to investigate regional responses. The corpus callosum was reported to be related to the abnormal interhemispheric functional connectivity and motor impairments (Chamard et al. 2016). Some concussion cases were reported to be related to the thalamus and basal ganglia (Grossman and Inglese 2016). The thalamus can transmit the information throughout the brain and join the communication with other brain regions, involving the multifunctional global pathways (Tang et al. 2011). In addition, the basal ganglia is critical for learning and memorizing (Graybiel 2000). Knowing the brain region-dependent functions, researchers have conducted studies on the responses of different brain components such as the corpus callosum, thalamus, and brainstem under impacts (Kleiven 2007; Patton et al. 2013; Post et al. 2017). For the corpus callosum, the strain tolerance was 0.28 and 0.31 (McAllister et al. 2012; Patton et al. 2013), and the tolerance for 50% likelihood ranged from 0.15 to 0.21 (Kleiven 2007; Patton et al. 2013; Zhang et al. 2004). For the thalamus, the strain tolerance ranged from 0.26 to 0.38 (Patton et al. 2013; Viano et al. 2005). Overall, the differences about the concussive threshold between the whole-brain and the deep-brain regions highlighted the importance of investigating how impacts affect the whole and the deep brain differently.

With the understanding that brain strains directly connect to brain damage, while head kinematics are currently used when developing protection gear, one major challenge is to systematically investigate the correlations between head kinematics and brain strains under complex impact scenarios. Below we reviewed commonly used kinematic magnitudes, impact directions, and linear/rotational impacts. We also reviewed rotational acceleration curve shapes and rotational deceleration.

Different impact locations induced various brain responses (Elkin et al. 2018; Zhang et al. 2001). Zhang et al. (2001) simulated frontal and lateral impacts to the brain and found that lateral impact produced higher shear stress than frontal impact did. Elkin et al. (2018) reported that the MPS and CSDM of the rear eccentric impacts were higher than those from other impacts. Hernandez et al. reported that the corpus callosum had high correlation to lateral impacts (Hernandez et al. 2019). However, impact direction is not equal to head kinematics. For example, a lateral impact to the face can induce a combination of head lateral bending and axial rotation. Hence, evaluating the influence of individual rotational direction, such as flexion/extension, lateral bending, and axial rotation, is beneficial to understand concussion.

The effects of linear and rotational kinematic on brain responses were studied. King et al. found that brain motion (± 1 mm) induced by linear acceleration was less than that induced by rotational acceleration (± 5 mm) (King et al.

2003). Zhang et al. (2004) reported that linear acceleration greatly affected intracranial pressure, and rotational acceleration greatly influenced shear stress. Kleiven (2007) also found that rotational kinematics had a higher correlation to the strain than translational kinematics did. Elkin et al. (2016) reported that there was a strong correlation between rotational kinematics and strain. Moreover, Post et al. found that the combination of linear and rotational acceleration could induce higher MPS than the pure rotational acceleration did within the first 10 ms of impacts (Post et al. 2017). Hence, investigating impacts with various combinations of linear and rotational kinematics is helpful to provide more evidence on the effect of rotational impacts.

Deceleration exists during the whole impact of football game (Newman et al. 1999). Both acceleration and deceleration can cause concussion (Newman et al. 1999). The process of deceleration was reported in the cadaver tests (Hardy et al. 2007). The deceleration loading curves were also studied (Kleiven 2007; Zhang et al. 2004). However, although brain responses to acceleration are widely studied (Pellman et al. 2003a; Post et al. 2017), brain responses to deceleration are not known, and need to be investigated.

The head kinematic loading curves consist of different shapes (Post et al. 2012; Rowson et al. 2009). The different shapes of the impact curves result in different brain responses. Zhao and Ji (2017) reported that the shape variation influenced the magnitude of the brain strain. Post et al. (2012) demonstrated that MPS and von Mises stress were influenced by the occasion of when the loading curves reached to the peak value, and the curves with longer duration before reaching the peak induced higher brain strains. Yoganandan et al. (2008) also revealed that brain strain was dependent on the load curve shapes. Hence, it's necessary to investigate the effects of curve shapes on the brain responses.

In this study, we comprehensively investigated the correlations between head kinematics and brain responses. For brain responses, we focused on CSDM (Gadd 1966; Tak-hounts et al. 2013; Versace 1971) to correlate to diffuse brain injuries, while peak strain or peak strain rate were not included. We conducted a total of 76 simulations to understand brain strains under various impacts. Our data revealed how well rotational velocity correlated to CSDM, under different impact directions, acceleration magnitudes, durations, decelerations, as well as loading curves with different shapes. Our data also showed how correlation was further changed when organizing impacts into different groups based on impact direction. Additionally, our data included rotational deceleration, which has not been addressed in existing kinematics-based injury threshold.

2 Method

2.1 Finite element model

The Global Human Body Model Consortium (GHBMC) head model including brain components such as the

cerebellum, brainstem, corpus callosum, basal ganglia and thalamus was used to evaluate brain responses (Fig. 2a, b). (Mao et al. 2013). The linear visco-elasticity material was used for both the gray matter and the white matter. The skull was defined as an elastic-plastic material with inner table, outer table, and trabecular layer (Mao et al. 2013). The model was validated against intracranial pressures and

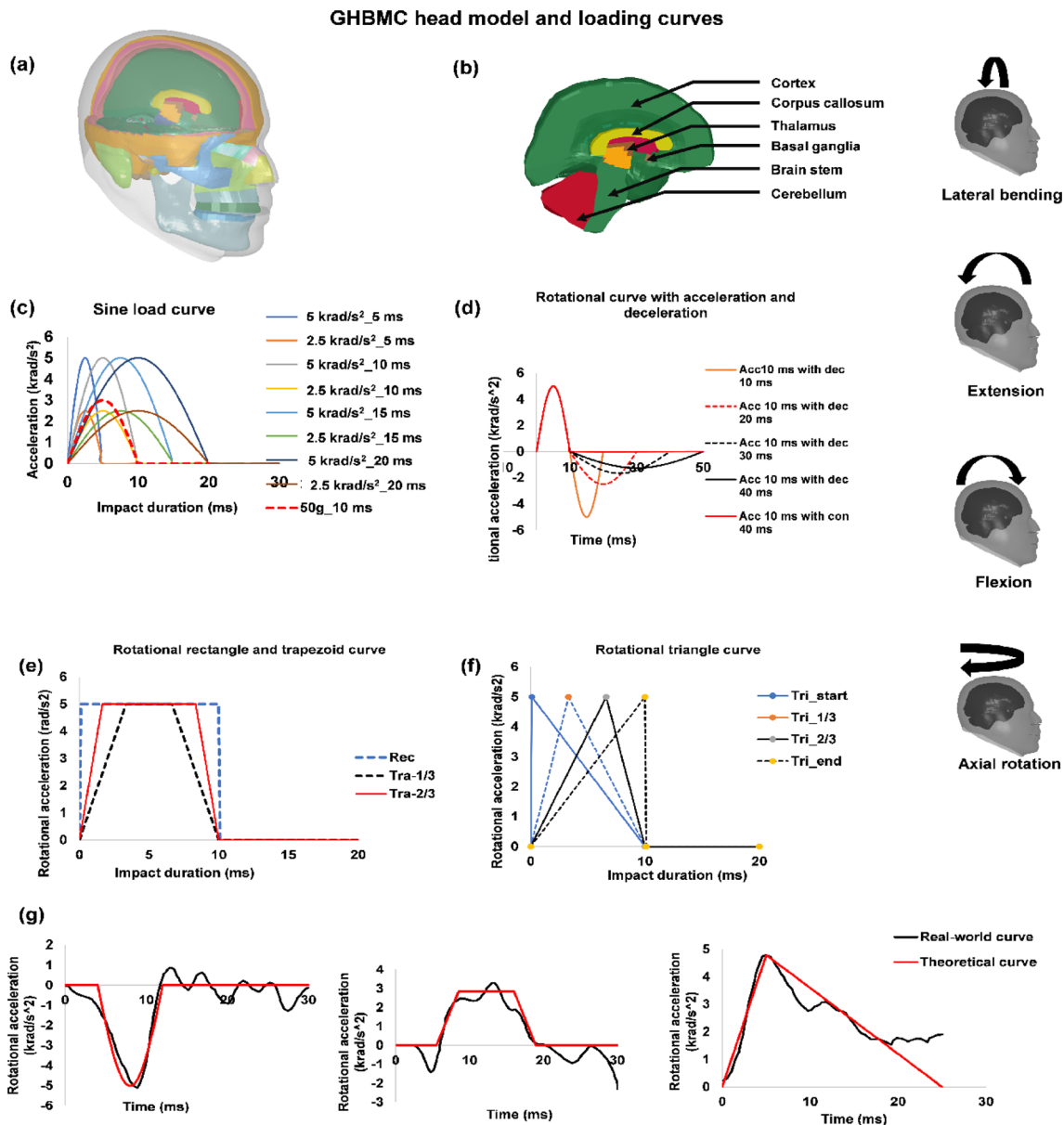


Fig. 2 The Global Human Body Model Consortium (GHBMC) head model and loading curves. **a** The head model; **b** The brain model; **c** Sine loading curve; 5 krad/s² indicates the peak acceleration was 5 krad/s², and 5 ms indicates impact duration. **d** Rotational loading curve with acceleration and deceleration; Acc indicates acceleration, and dec indicates deceleration. **e** Rotational rectangle and trapezoid load curve; Rec indicates rectangle curve; Tra-1/3 indicates trapezoid curve with the peak acceleration occupying 1/3 of the

duration; Tra-2/3 indicates trapezoid curve with the peak acceleration occupying 2/3 of the duration. **f** Rotational triangle curve; Tri-start indicates triangle curve peaking at the start of the curve; Tri-1/3 indicates triangle curve peaking at the 1/3 of the curve; Tri-2/3 indicates triangle curve peaking at the 2/3 of the curve; Tri-end indicates triangle curve peaking at the end of the curve. **g** Schematic drawings showing how theoretical curves were based on real-world kinematics (Pellman et al. 2003b; Zhang et al. 2004)

brain displacements (Hardy et al. 2001; Nahum et al. 1977; Trosseille et al. 1992).

2.2 Description of linear and rotational curves

The linear and rotational acceleration time history curves were imposed to the center of gravity of the GHBMC head model with the “Boundary_Prescribed_Motion”. The sinusoidal curves were used for the linear and rotational impacts. For 32 pure rotational impact simulations, we defined two peak magnitudes (2.5 and 5 krad/ms²) based on Fig. 1, and four acceleration durations levels (5, 10, 15 and 20 ms) with additional 10 ms afterwards respectively (Fig. 2c). All these two magnitudes and four levels were applied to four impact directions, yielding 32 cases. For four combined linear and rotational cases, the rotational acceleration curve with peak magnitude of 5 krad/ms² and duration of 10 ms was combined with the linear acceleration curve with peak magnitude of 50 g and duration of 10 ms to explore brain strains. For 12 cases related to rotational deceleration, the peak rotational acceleration of 5 krad/ms² and positive duration of 10 ms was used, combined with four levels of deceleration duration (10, 20, 30 and 40 ms) (Fig. 2d), providing the exact same rotational velocity and same duration when studying deceleration effect. These four levels of deceleration were applied to three impact directions (lateral bending, extension and axial rotation), yield 12 cases. For 28 cases related to curve shapes, seven curve shapes (Fig. 2e and f) beside sinusoidal shape were applied in four impact directions. The curve shapes included rectangle, trapezium, and triangle, all with the peak acceleration of 5 krad/s² and the acceleration duration 10 ms. Two kinds of trapezoid curves with the peak acceleration occupying the 1/3 and 2/3 of the acceleration duration respectively (Fig. 2e) were selected. Four kinds of the triangle curves were applied with the peak acceleration point reaching at the start, 1/3, 2/3 and the end of the whole acceleration duration (Fig. 2f).

2.3 Analysis method

MPS contour, CSDM value, and average strain were used to demonstrate simulation result. The results of CSDM20, which represents the percentage of the elements for which the strain is higher than 0.20, were primarily presented for analysis while the results of other CSDM levels are listed in “Appendix A”, because 0.20 was suggested as a strain threshold of concussion (Kleiven 2007; Zhang et al. 2004). The relative mean difference (RMD) (Eq. 1) (Rush et al. 2017) was used to show the difference between linear-with-rotational and rotational-only groups. The CSDM difference (Eq. 2) was used to show the difference between with-deceleration group and without-deceleration group. Regression

analysis was used to analyze the correlation between the CSDM values and velocities.

$$\text{RMD} = \frac{\text{CSDM.LR} - \text{CSDM.R}}{\text{CSDM.R}} \quad (1)$$

where RMD is relative mean difference, CSDM.LR is CSDM from impacts with both linear and rotational accelerations, CSDM.R is CSDM from impacts with rotational acceleration.

$$\text{CSDM difference} = \frac{\text{CSDM.w.d} - \text{CSDM.wo.d}}{\text{CSDM.wo.d}} \quad (2)$$

where CSDM.w.d is CSDM from impacts with rotational deceleration, CSDM.wo.d is CSDM from impacts without rotational deceleration.

For analyzing the correlation between peak rotational velocity and CSDM values under specific subgroups, a Pearson’s analysis based on Excel was adopted. The same correlation analysis was adopted to analyze the correlation between CSDM and average strain. For analyzing the correlation between peak rotational acceleration/velocity and CSDM/average strain while considering the effect of impact duration, impact direction, and loading curve shape, SPSS (Version 26, IBM Corporation, Somers, NY, USA) was adopted with R^2 values for predictors of acceleration and velocity being compared.

3 Results

3.1 Brain strain distribution due to rotational impact

For the whole brain, axial rotation induced the largest MPS distribution with most of the added strains shown in the deep cortex region, followed by extension & flexion and lateral bending (Fig. 3). For example, among impacts with duration of 10 ms, CSDM20 from axial rotation was calculated as 0.41, followed by the CSDM20 of 0.23 from both flexion and extension which produced similar strain loading (Fig. 4a). The CSDM20 result of lateral bending was the lowest (Fig. 4a) as 0.16.

For the corpus callosum, lateral bending produced highest CSDM values among all CSDM levels, followed by the CSDM values induced by axial rotation. Flexion and extension produced the lowest CSDM values (Fig. 4b). With impact duration 10 ms, CSDM20 value produced by lateral bending and axial rotation were 0.39 and 0.28, respectively. Mostly, CSDM20 values produced by extension were higher than those produced by flexion except for the condition of impact duration 20 ms.

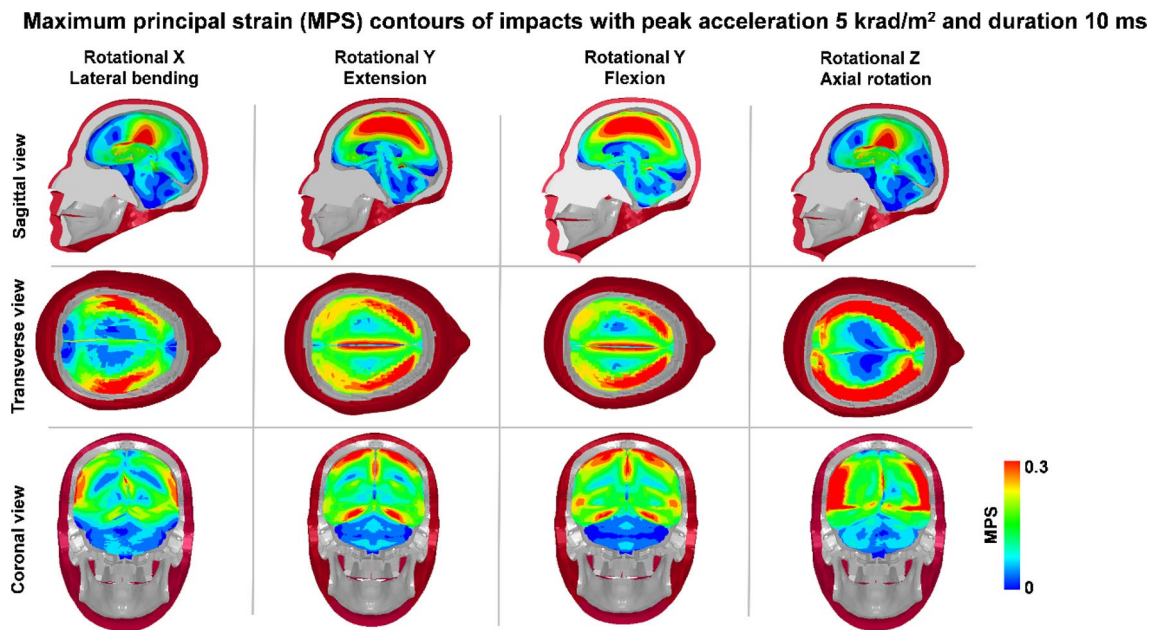


Fig. 3 Maximum principal strain (MPS) contours of impacts with peak acceleration 5 krad/s² and duration 10 ms. Three views (sagittal, transverse and coronal) of the MPS contours were plotted with the range between 0 and 0.3

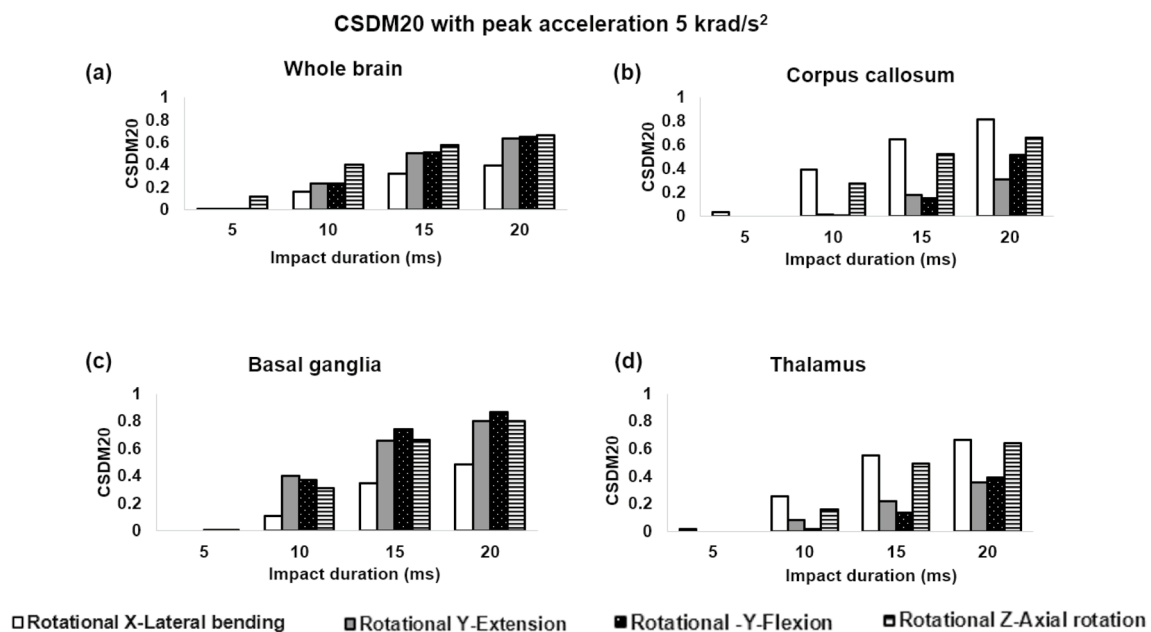


Fig. 4 CSDM20 of different brain regions under different impacts. **a** CSDM20 for the whole brain; **b** CSDM20 for the corpus callosum; **c** CSDM20 for the basal ganglia; **d** CSDM20 for the thalamus

For the basal ganglia, overall, the CSDM values produced by flexion and extension were highest, followed by those produced by axial rotation and lateral bending (Fig. 4c). The CSDM values induced by flexion and extension were slightly different depending on CSDM levels. For CSDM20 within impact duration 10 ms (Fig. 4c), the values induced

by flexion, extension, axial rotation and lateral bending were 0.4, 0.37, 0.31 and 0.11 respectively.

For the thalamus, interestingly, lateral bending, which produced the lowest CSDM within the whole brain, induced the highest CSDM in this deep-brain region (Fig. 4d), followed by axial rotation, flexion and then extension. With

impact duration of 10 ms, lateral bending, axial rotation, extension and flexion produced CSDM20 of 0.25, 0.16, 0.08, and 0.01.

3.2 CSDM relative mean difference (RMD) between impacts of the combination of linear and rotational accelerations and pure rotational acceleration

Generally, except for the case with combined lateral bending and translational motion, the RMD that indicates the relative mean difference did not change obviously, only with the increase within 1% (Table 1). Even for the case with combined lateral bending and translational model, the absolute differences of CSDM were less than 0.03.

3.3 The effect of deceleration

Overall, large difference existed when deceleration was considered. Rotational deceleration in axial rotation mode produced highest changes to CSDM among all three directions (27% increase of CSDM20) (Fig. 5). The CSDM difference with other strain levels were listed in “Appendix B”. Rotational deceleration in lateral bending mode and extension mode also affected CSDM. Interestingly, deceleration reduced CSDM values when deceleration durations were short (≤ 10 ms for all loading modes and ≤ 20 ms for the extension loading mode) and increased CSDM values when deceleration durations were long (≥ 20 ms for lateral bending and axial rotation loading modes, ≥ 30 ms for extension loading mode).

3.4 The effects of loading curves with different shapes

The rectangular shape loading curves induced the highest CSDM value, with CSDM20 of 0.62, 0.55 and 0.37 under axial rotation, flexion and extension, and lateral bending, respectively (Fig. 6). The trapezoid curve with the peak

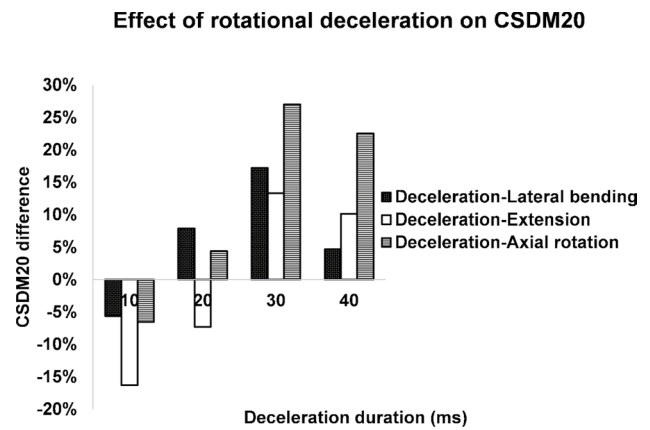


Fig. 5 Effect of rotational deceleration on CSDM20

acceleration occupying 2/3 of duration caused the second largest strain distribution (Fig. 6). Axial rotation induced CSDM20 of 0.54, which was the highest among all impacts. The impacts with the trapezoid curve with peak acceleration occupying 1/3 of the duration produced the third highest CSDM20 values, with CSDM20 of 0.43 induced by the axial rotation, CSDM20 of 0.27 generated by flexion and extension, and CSDM20 of 0.18 under lateral bending (Fig. 6). The CSDM20 values from the sine-curve loading and from the trapezoid-curve loading with peak acceleration of 1/3 of the duration were similar (Fig. 6). The lowest CSDM20 results were from the triangular curves (Fig. 6). Among the four triangle shapes, overall the CSDM values were close. However, the triangle-curve loading with acceleration peaking at 2/3 of duration produced the highest value, while the triangle-curve loading with acceleration peaking at the beginning generated the lowest (Fig. 6).

Table 1 CSDM relative mean difference (RMD) for impacts with combined of linear and rotational acceleration and impacts with rotational acceleration

CSDM level	0.1	0.15	0.2	0.25	0.3
Linear X and flexion (rotational-Y) versus flexion	0.14% (0.7409 vs. 0.7399)	0.29% (0.4687 vs. 0.4673)	0.74% (0.2366 vs. 0.2348)	0.40% (0.0930 vs. 0.0926)	0.57% (0.0396 vs. 0.0394)
Linear-X and extension (rotational Y) versus extension	0.08% (0.7254 vs. 0.7249)	0.37% (0.4597 vs. 0.4580)	0.66% (0.2371 vs. 0.2355)	0.85% (0.0963 vs. 0.0955)	0.31% (0.0383 vs. 0.0382)
Linear Y and lateral bending (rotational X) versus lateral bending	2.67% (0.6017 vs. 0.6182)	7.09% (0.3361 vs. 0.3617)	8.78% (0.1471 vs. 0.1613)	12.98% (0.0565 vs. 0.0649)	25.44% (0.0180 vs. 0.0241)
Linear Y and axial rotation (rotational Z) versus axial rotation	0.67% (0.8808 vs. 0.7955)	0.91% (0.5922 vs. 0.5868)	0.33% (0.4066 vs. 0.4052)	0.41% (0.2671 vs. 0.2682)	0.75% (0.1678 vs. 0.1690)

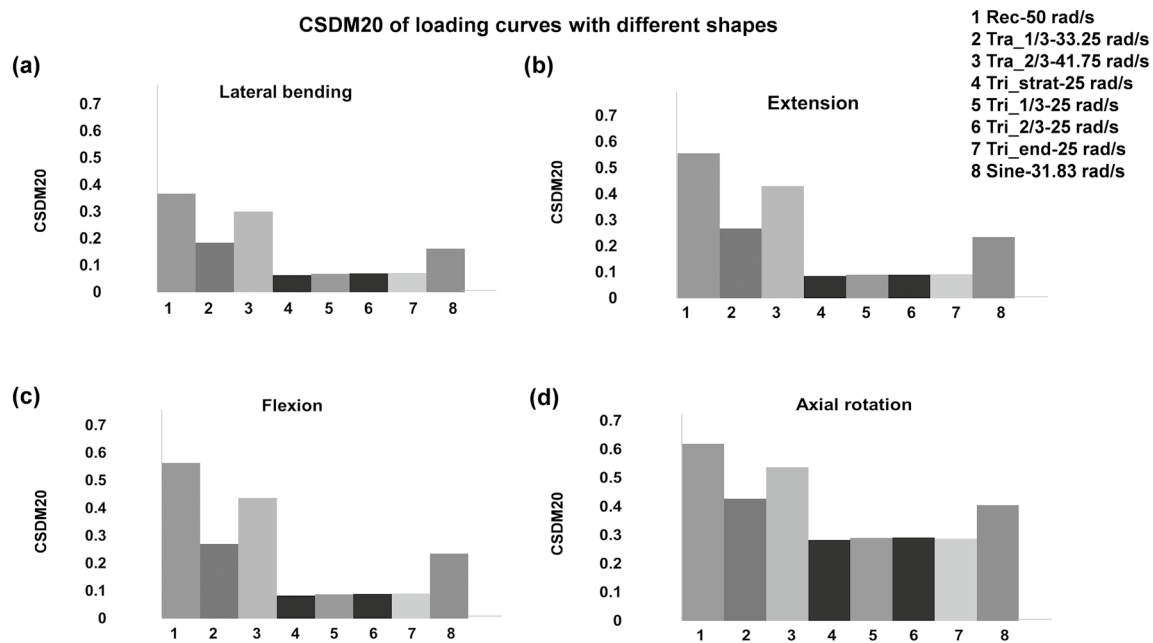


Fig. 6 CSDM20 of impacts with loading curves with different shapes. **a** CSDM20 of loading curve with different shapes under lateral bending. **b** CSDM20 of loading curve with different shapes under extension. **c** CSDM20 of loading curve with different shapes under flexion. **d** CSDM20 of loading curve with different shapes under axial rotation. For the legend, Rec indicates rectangle curve, and its integrated velocity was 50 rad/s; Tra-1/3 indicates trapezoid curve with the peak impulse occupying 1/3 of the duration, and its integrated velocity was 33.25 rad/s; Tra-2/3 indicates trapezoid curve with the peak

impulse occupying 2/3 of the duration, and its integrated velocity was 41.75 rad/s; Tri-start indicates triangle curve peaking at the start of the duration, and its integrated velocity was 25 rad/s; Tri-1/3 indicates triangle curve peaking at the 1/3 of the duration, and its integrated velocity was 25 rad/s; Tri-2/3 indicates triangle curve peaking at the 2/3 of the duration, and its integrated velocity was 25 rad/s; Tri-end indicates triangle curve peaking at the end of the duration, and its integrated velocity was 25 rad/s; Sine indicates sine curve with integrated velocity of 31.83 rad/s

3.5 Correlation between rotational velocity and CSDM

Correlations between CSDM and kinematics are shown in Fig. 7. For sine-shape rotational velocity loadings with different peak accelerations (2.5 and 5 krad/s²) and different impact durations (5, 10, 15 and 20 ms), rotational velocities highly correlated with CSDM20 with R^2 all above 0.94 for four directions (lateral bending, extension, flexion, and axial rotation) groups (Fig. 7a). For other CSDM levels, most of R^2 values were above 0.9 (“Appendix C”). When considering different shapes (Fig. 2c and d), R^2 values also reached to very high numbers above 0.99 for four direction groups (Fig. 7c), while the variances of CSDM20 under same peak acceleration varied dramatically, ranging from 0.01 to 0.67 (Fig. 7b). CSDM/average strain correlated well to peak rotational velocity with R^2 values ranging from 0.71 to 0.82 with an average of 0.77 (Fig. 7d), while CSDM/average strain correlated poorly to peak acceleration with R^2 values ranging from 0.14 to 0.35 (Fig. 7d). Between CSDM and average strain, there existed strong correlations with R^2 values ranging from 0.85 to 0.95 (Fig. 7e).

4 Discussion

4.1 CSDM of different brain regions due to rotational impact

The axial rotation produced the highest CSDM within the whole brain. Similar results were found in other CSDM levels (“Appendix A”). Our finding is consistent with Elkin et al.’s observation, which reported that eccentric impacts (induced axial rotation) produced higher strains compared to jaw impacts (Elkin et al. 2018). Zhang et al. (2001) found that lateral-bending impacts produced the higher shear stress levels than frontal impacts, while we found that flexion and extension caused higher CSDM values than that of lateral bending. We also found that flexion and extension produced similar strain levels in brain tissue. However, Krave et al. (2011) subjected rabbits under rotational loadings and found that flexion induced more brain injury than extension did. The geometrical difference of head structure between human and rabbit may contribute to differences between our and Krave et al.’s results. Lateral bending produced the lowest strain level, possibly because stiff falx and tentorium

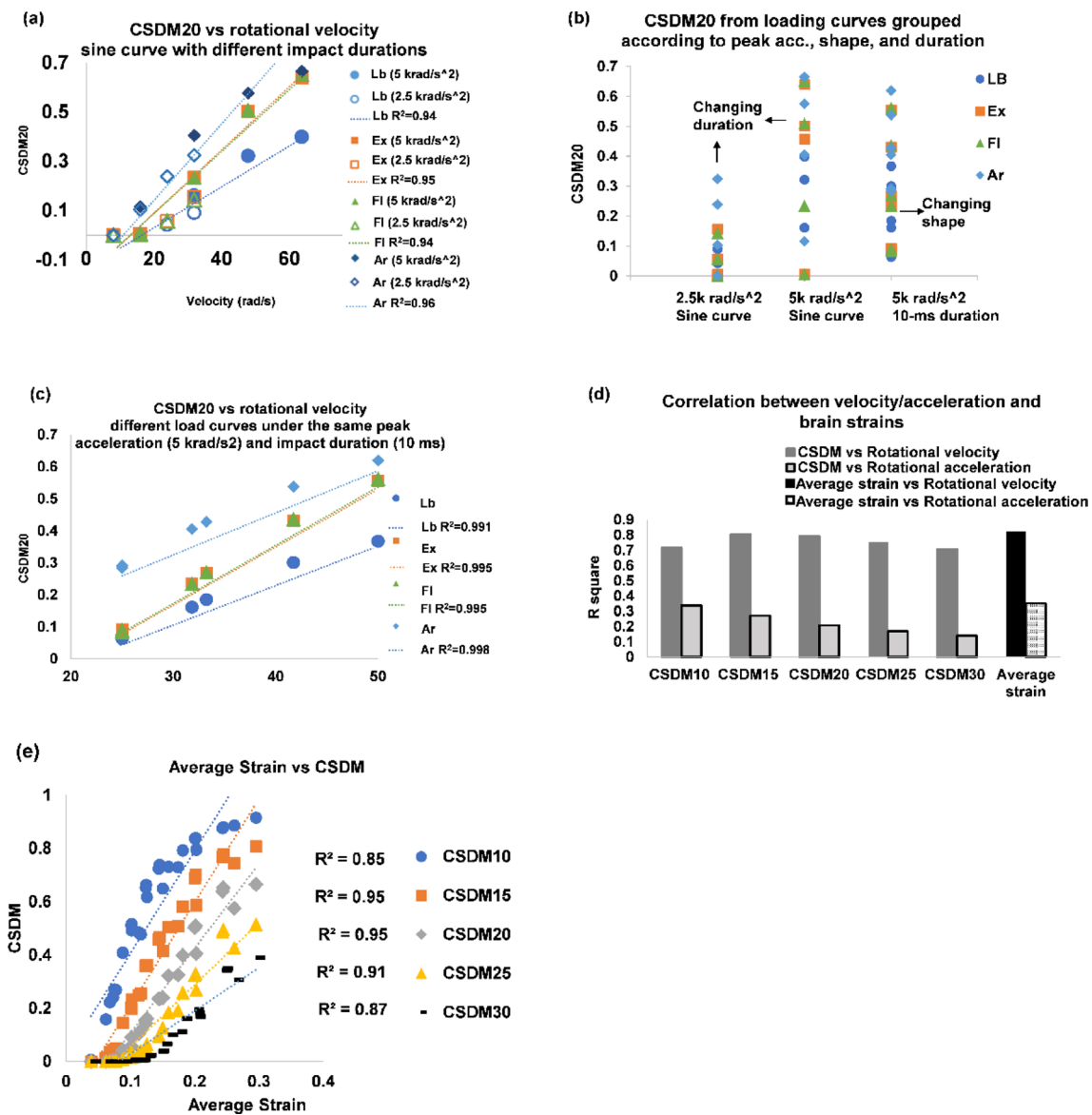


Fig. 7 Correlation between CSDM/average strain and rotational kinematics. **a** Correlation between CSDM and peak rotational velocity under sine curve with different impact durations; **b** CSDM20 compared to peak rotational acceleration with different loading curves under the same peaking acceleration (5 krad/s²) and impact duration (10 ms); **c** Correlation between CSDM20 and peak velocity with dif-

ferent loading curves under the same peaking acceleration (5 krad/s²) and impact duration (10 ms); **d** R² values between rotational peak velocity/acceleration and CSDM/average strain; **e** correlation between CSDM and peak rotational velocity. *Lb* Lateral bending, *Ex* extension, *Fl* flexion, *Ar* axial rotation

prevented the brain from deforming much. Our results supported developing the brain injury criteria considering direction effects (Takhounts et al. 2013).

Kleiven (2007) reported that the threshold of CSDM10 of 50% possibility injury risk for the white matter was 0.47. In addition, Kleiven (2005) reported that over 0.5 MPS appeared in the corpus callosum under axial rotation. Our data showed that CSDM10 values of the corpus callosum, the basal ganglia and the thalamus which belong to white matter were different under different impact directions. Since

brain responses to different brain regions under various directional impacts were different, it is ideal to consider different brain regions when investigating brain injury criteria.

4.2 The influence of linear acceleration

The tiny influence was imposed by the linear kinematics when it was combined with the rotational kinematics. Based on our results (Table 1), the slight change of CSDM existed when the linear impact was combined with rotational impact

being compared to the rotational impact alone. Most of RMD values which indicate the difference of the strain produced by combination of linear and rotational impacts and pure rotational impacts were around 1%, consistent with Table 1. Our result is consistent with findings of other groups. King et al. (2003) demonstrated that the rotational acceleration would be the essential cause of brain strain. Kleiven (2007) showed that rotational kinematics was important to brain deformation. Interestingly, we also found that when forward linear motion was combined with lateral bending, brain strain was slightly lower than that produced by the pure lateral bending. It should be mentioned that although the percentile differences for CSDM0.25 and CSDM0.3 were large as 12.98% and 25.44% when introducing linear acceleration in lateral bending case, the absolute differences of CSDM values were only 0.008 and 0.006, respectively. Overall, the influence of linear acceleration on brain strain was small and can be neglected.

4.3 The role of rotational deceleration

We found that the brain responses in the cases with and without the rotational deceleration were different. The

CSDM values of the cases with deceleration were higher than those without deceleration when the deceleration durations were equal to and larger than 30 ms (Fig. 5), while the CSDM values of impacts with deceleration was lower than that without deceleration when the deceleration durations were within 20 ms. While such a nonlinear deceleration effect seemed not straightforward, we further analyzed strain development and found that 10-ms rotational deceleration could cancel some brain strains (Fig. 8), while 30-ms or 40-ms rotational deceleration did not cancel much strain but introduced more strains at a later time around 36 ms (Fig. 8). Interestingly, Sanchez et al. used real-world head kinematics curves, which included deceleration phase, and highlighted the importance to solve impact simulations long enough to represent brain strain development (Sanchez et al. 2018). Our results demonstrated the importance of deceleration duration. We also found that axial rotation with deceleration phase induced the highest CSDM difference compared to that without deceleration (the highest CSDM difference reached to 50%) (“Appendix B”). Moreover, with the same deceleration loading curves, the axial rotation produced higher CSDM difference than the lateral bending and extension did. Considering rotational deceleration will be

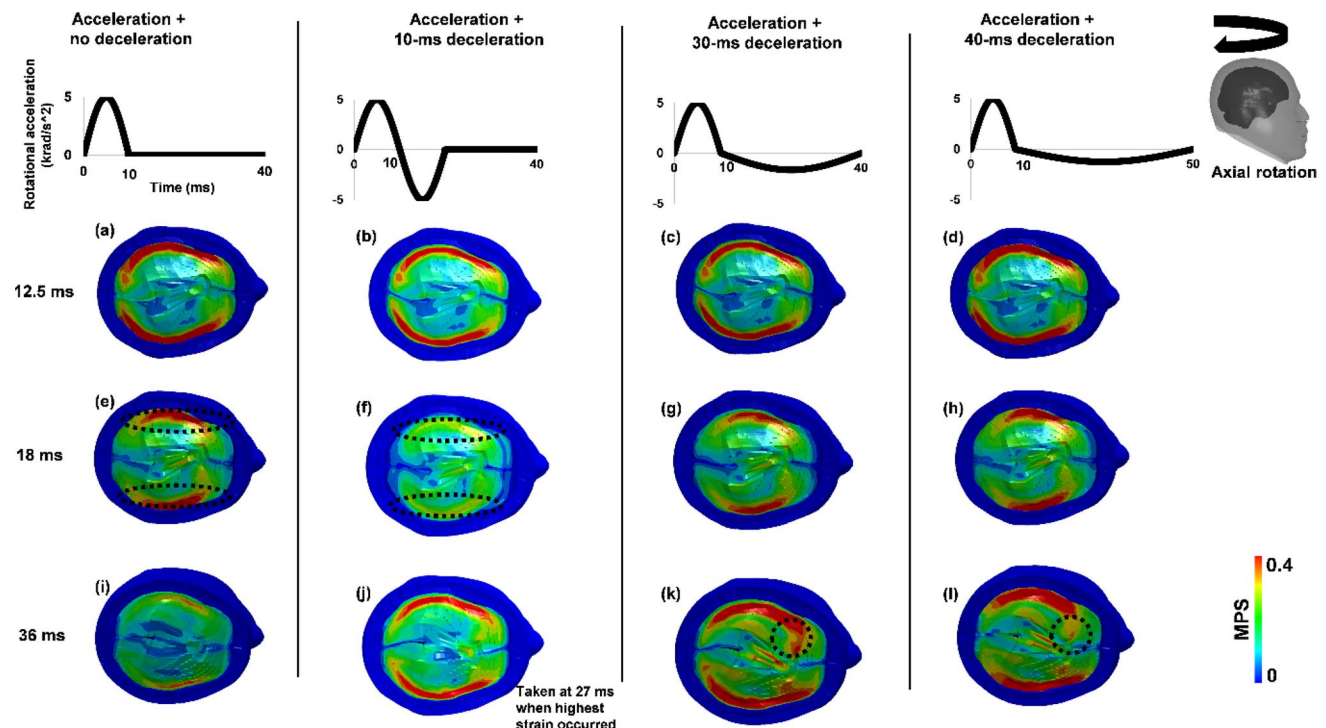


Fig. 8 Brain strain contours in baseline, no rotational deceleration loading and loadings with various rotational deceleration durations. The first occurrence of high brain strains remained similar for all four loading conditions (a–d). The 10-ms deceleration cancelled out some of brain strains developed at around 18 ms (comparing e–f). Such a cancellation effect was less obvious using prolonged deceleration curves (g and h). All deceleration curves induced large brain strains

during 25–40 ms (j–l) while baseline, no-deceleration condition did not introduce additional high strains during the same time period (i). Moreover, 30-ms deceleration loading condition induced most “s” shape brain deformation and induced high strains at 36 ms (k), which were larger than the first occurrence of strains (c). The 40-ms deceleration loading also induced high strains at 36 ms, but less in the frontal brain region (l) compared to the 30-ms deceleration case did (k)

critical for developing a more effective rotational-velocity-based brain injury criteria. Meanwhile, caution needs to be practiced when using head form only for helmet test as the deceleration from neck constraints will be missing during such a setting.

4.4 The effects of loading curve shapes

Brain strains varied when loading curve shapes changed under rotational accelerations with the same peak and duration. Generally, the rectangular curve induced the largest strain distribution, while the triangular curve produced the lowest strain distribution. This is due to the velocity integrated from the rectangular curve was higher than that of the triangular curve. The integrated velocity of rectangular curve was 50 rad/s, higher than that integrated from the triangular curve which was 25 rad/s (Fig. 6). Hence, higher rotational velocity calculated out of loading curves produced higher strain distributions. The same reason can also be used to explain why the trapezoid curve with the peak acceleration occupying 2/3 of the duration produced the second largest strain distribution, followed by that with the peak acceleration occupying 1/3 of the duration, and the sine curve. For the four triangular loading curves, with the same integrated rotational velocity of 25 rad/s, CSDM produced by the triangular curve with the acceleration peaking at 2/3 of duration was 0.01 higher than CSDM from the other three loadings. Moreover, Post et al. used the loading curves which is similar to the sine curve and reported that the loading curve with the acceleration peaking lately produced higher strain responses (Post et al. 2012). However, we found that based on the same integrated rotational velocity, the curves with the acceleration peaking at 2/3 rather than the end of the duration produced slightly larger strain distribution (Fig. 6). The differences between two groups could be partially due to the use of different human head models.

4.5 The correlation between rotational velocity and CSDM

We found there existed strong correlations between CSDM and rotational velocity but weak correlation between CSDM and rotational acceleration. Under the curves with the same shape (sine curve), different peak accelerations and durations under specific directions, the lowest R^2 of rotational velocity and CSDM20 reached to 0.94 (Fig. 7a), which indicates that under a specific impact direction and a load curve shape, the correlation between CSDM and the rotational velocity is strong regardless of different impact durations. This correlation remained strong when loading curves with different shapes were considered (Fig. 7c). Takhounts et al. also reported good correlation between max resultant rotational

velocity and CSDM (R^2 of 0.91) (Takhounts et al. 2013). When grouping all directions as well as the peak accelerations, durations and load curve shapes, correlations between CSDM and rotational velocity decreased but still not low with R^2 between 0.70 and 0.80 (Fig. 7d), while R^2 of CSDM and rotational acceleration was within the range of 0.30–0.40 (Fig. 7d). Knowles et al. reported that there existed the high correlation (R^2 of 0.86) between the change of resultant rotational velocity and CSDM15 with the consideration of different impact locations of helmet (Knowles and Dennison 2017). Our data showed that the R^2 of rotational velocity and CSDM15 was 0.80 when impact directions and load curve with different shapes were considered (Fig. 7d). Gabler et al. stated that brain deformation mainly depended on rotational velocity in short-duration impacts, but it depended more on the rotational acceleration in long-duration impacts (Gabler et al. 2018). The cases we studied were based on the events of sports-related concussion, for which the durations were no more than 30 ms. It can be specified that based on our study with impact durations 5–20 ms, velocity correlates well to CSDM. Together with the literature, our study supported the use of rotational velocity instead of acceleration as a predictor of brain injury for impacts with a major positive phase lasting equal to and less than 20 ms.

4.6 Limitations

To sort out the effect of peak rotational acceleration, duration, peak rotational velocity, shape of loading curve, and rotational deceleration on brain strains, theoretical loading curves were used. It should be acknowledged that differences in brain strain prediction between a real-world loading curve and a simplified theoretical curve existed (“Appendix D”). Another limitation is that the accuracy of using the brain model for predicting deep strains still needs to be further validated. Various gray and white matter parts were assigned with one type of gray matter material and one type of white-matter material. Further cadaver human brain material tests will help improve the accuracy of model predictions. Nevertheless, using one of the most extensively validated brain model and real-world-based theoretical curves, this study quantified the effects of deceleration curve, shape, direction, peak rotational acceleration and peak rotational velocity, with part of findings being verified by comparing to simulation results from real-world kinematic curves (such as in “Appendix D”).

5 Conclusions

We systematically investigated how head kinematics—which included various rotational magnitudes (2.5 and 5 krad/s²), linear plus rotation, various durations (15, 20, 25 and

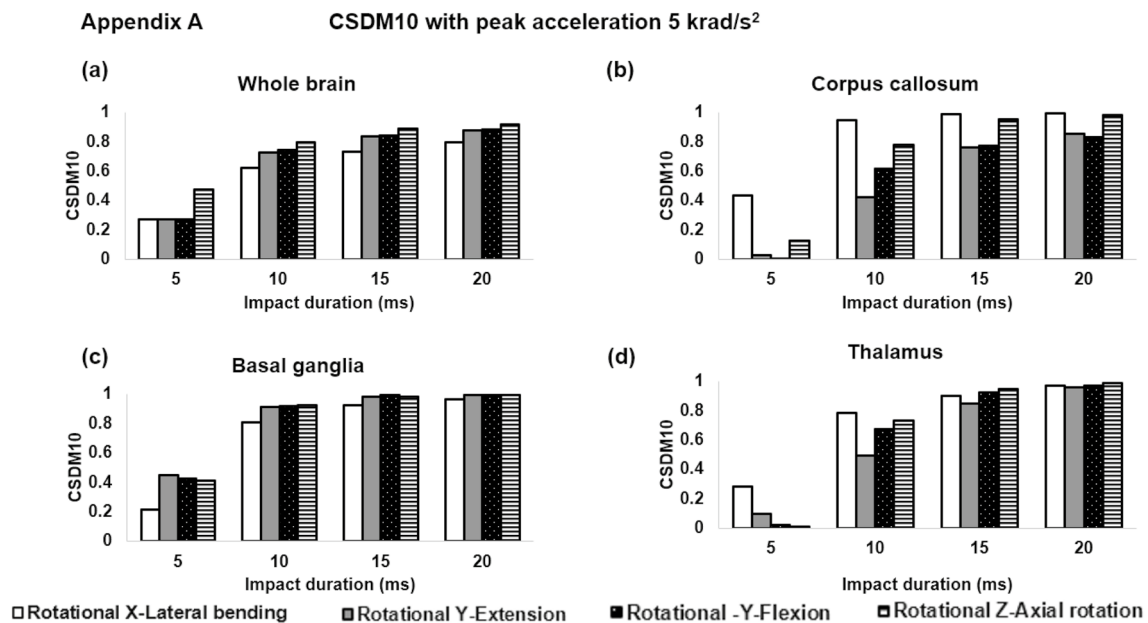
30 ms), with and without deceleration, various loading curve shapes—affected brain strains. We found that axial rotation produced highest strain loading to the whole brain while lateral bending produced lowest strain. Meanwhile, the same lateral bending produced highest strain to the corpus callosum and the thalamus. Flexion and extension produced similar, middle-level strains to the whole brain, while they produced highest strains to the basal ganglia. These various effects of impact direction on the whole-brain and deep-brain structures are important for concussion prevention as deep brain structures have been suggested to be concussion relevant. Our data also concurred with the literature that rotation is the main cause of brain strains (over 99%). Furthermore, our data highlighted the importance of rotational deceleration and found that shorter deceleration duration of 10 ms reduced CSDM20 up to 17% while longer

deceleration duration of 30 ms increased CSDM20 up to 27%. Such finding suggests the potential of optimizing deceleration with a short duration for future protection gear design. Lastly, our data demonstrated that rotational velocity, rather than rotational acceleration, correlated to brain strains with an average R^2 of 0.77 across various impact directions and different shapes of loading curves. When grouping impacts to four direction groups, the correlation between rotational velocity and brain strain reached to an average R^2 above 0.94, including various loading curve shapes.

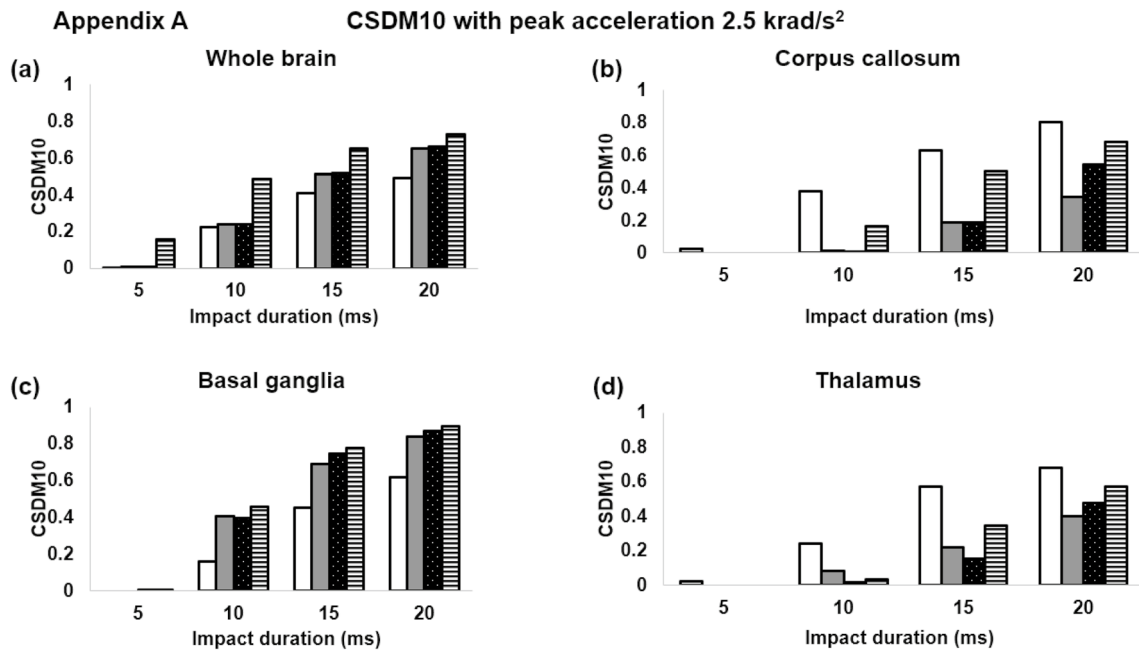
Acknowledgements We acknowledge the Canada Research Chairs program (X2281B63) and NSERC (R5748A04) for support. We acknowledge Dr. Youcai Wu and Dr. Cheng-Tang Wu from LSTC for their help with data analysis. We acknowledge Mr. Yanir Levy for the support in statistical analysis.

Appendix A: Results of CSDM10, CSDM15, CSDM20, CSDM25, and CSDM35 for various peak accelerations and rotational directions

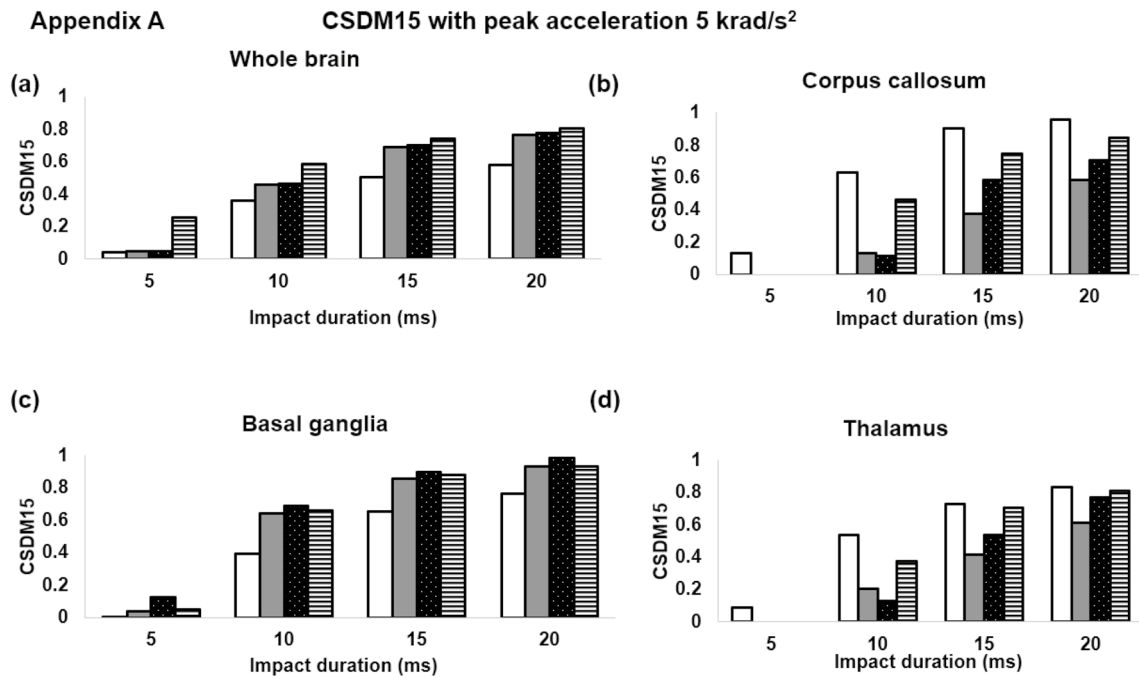
Results of CSDM10 for peak acceleration 5 krad/s².



Results of CSDM10 for peak acceleration 2.5 krad/s².

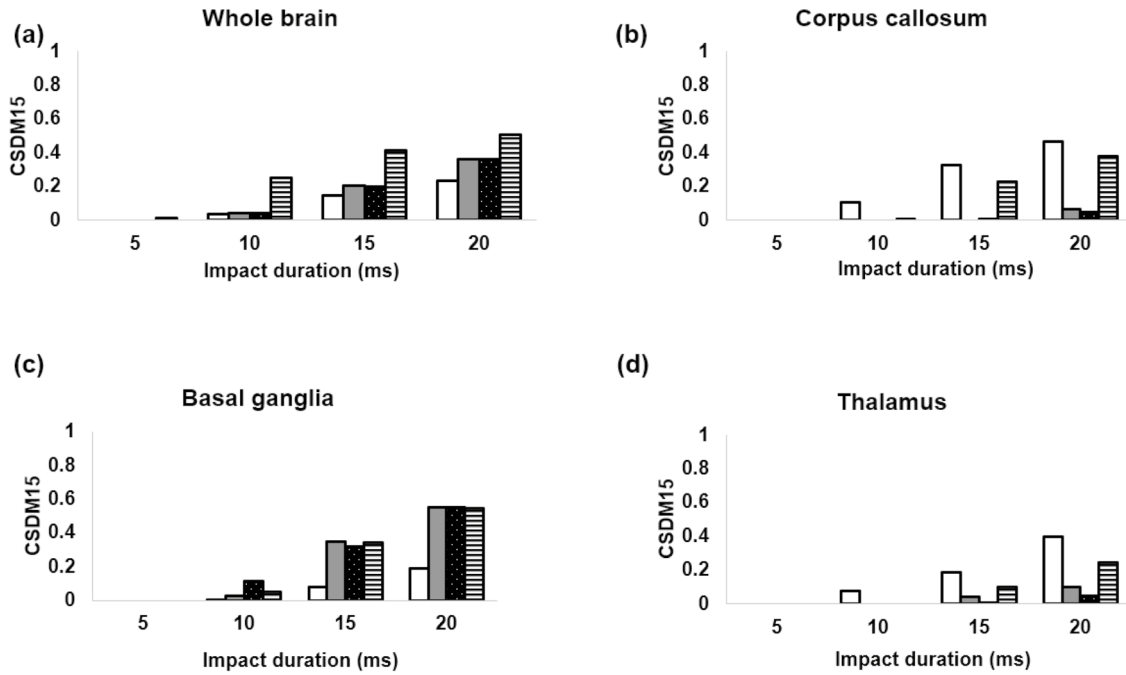


Results of CSDM15 for peak acceleration 5 krad/s².



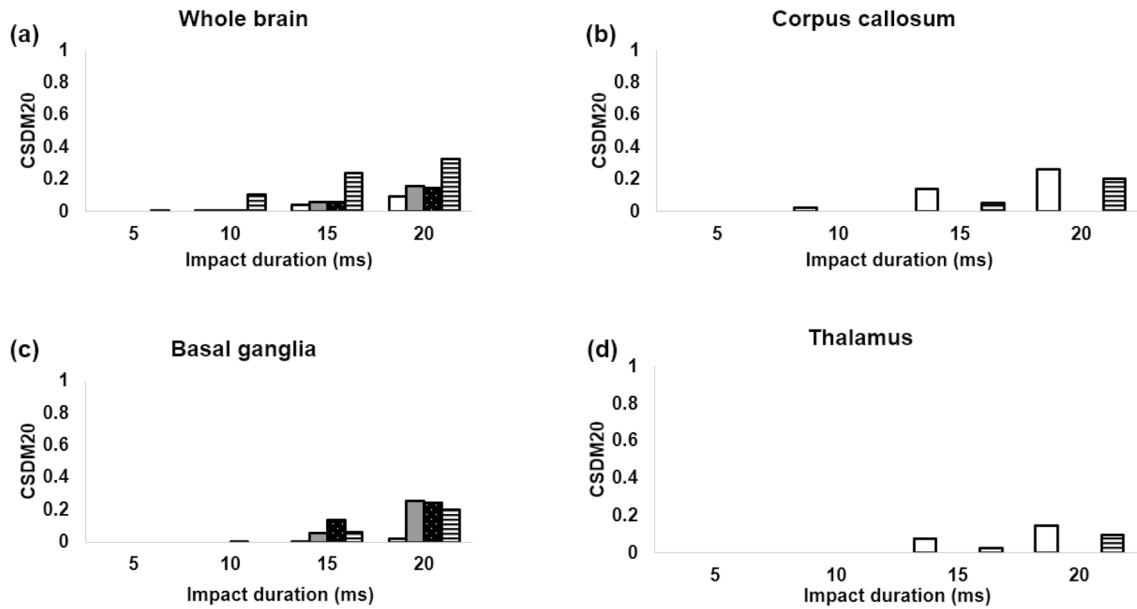
Results of CSDM15 for peak acceleration 2.5 krad/s².

Appendix A CSDM15 with peak acceleration 2.5 krad/s²

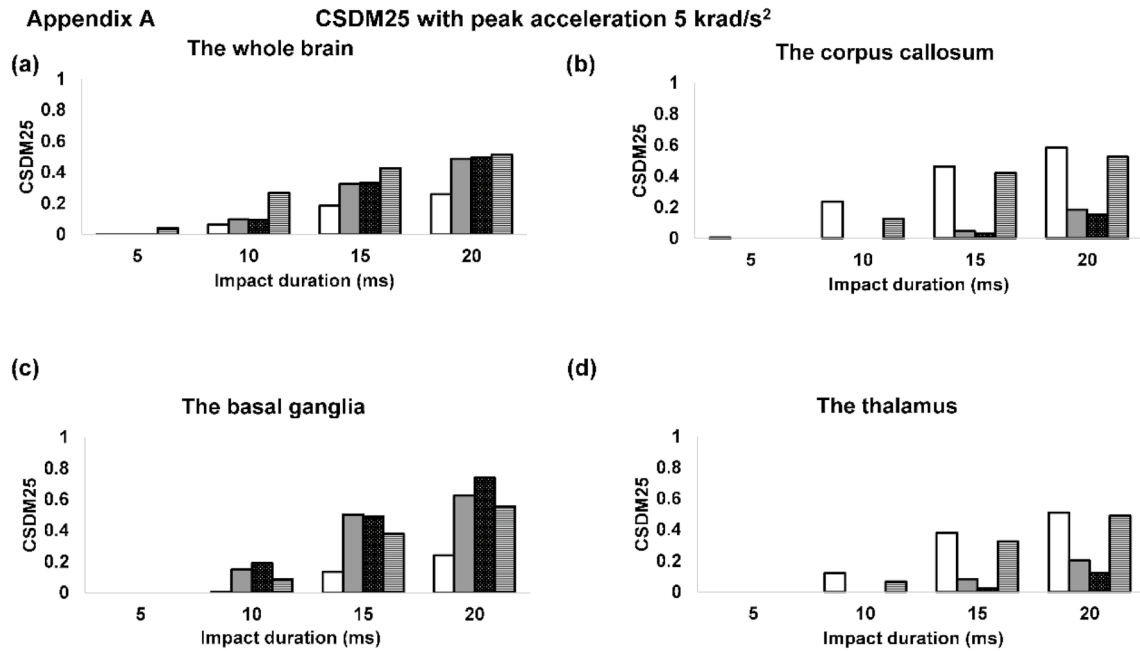


Results of CSDM20 for peak acceleration 2.5 krad/s².

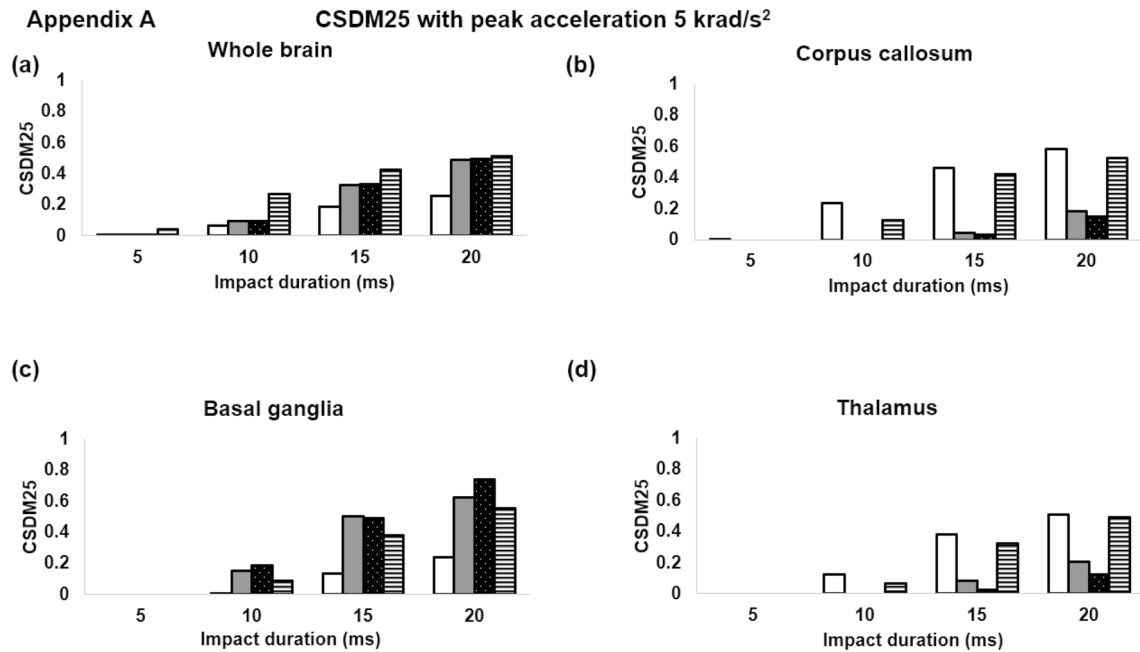
Appendix A CSDM20 with peak acceleration 2.5 krad/s²



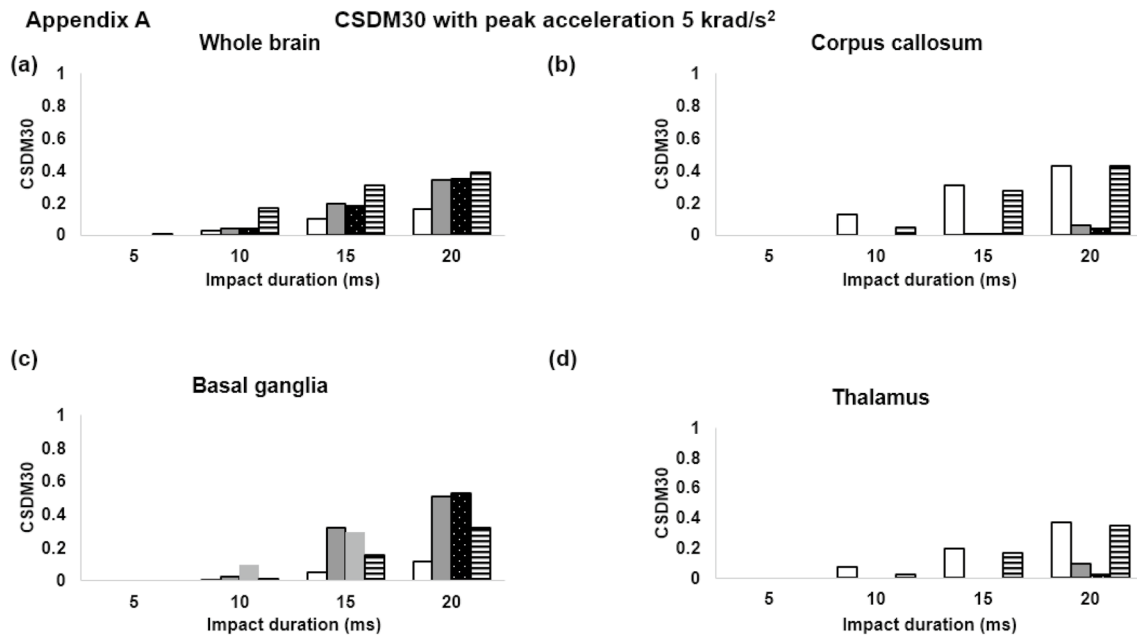
Results of CSDM25 for peak acceleration 5 krad/s².



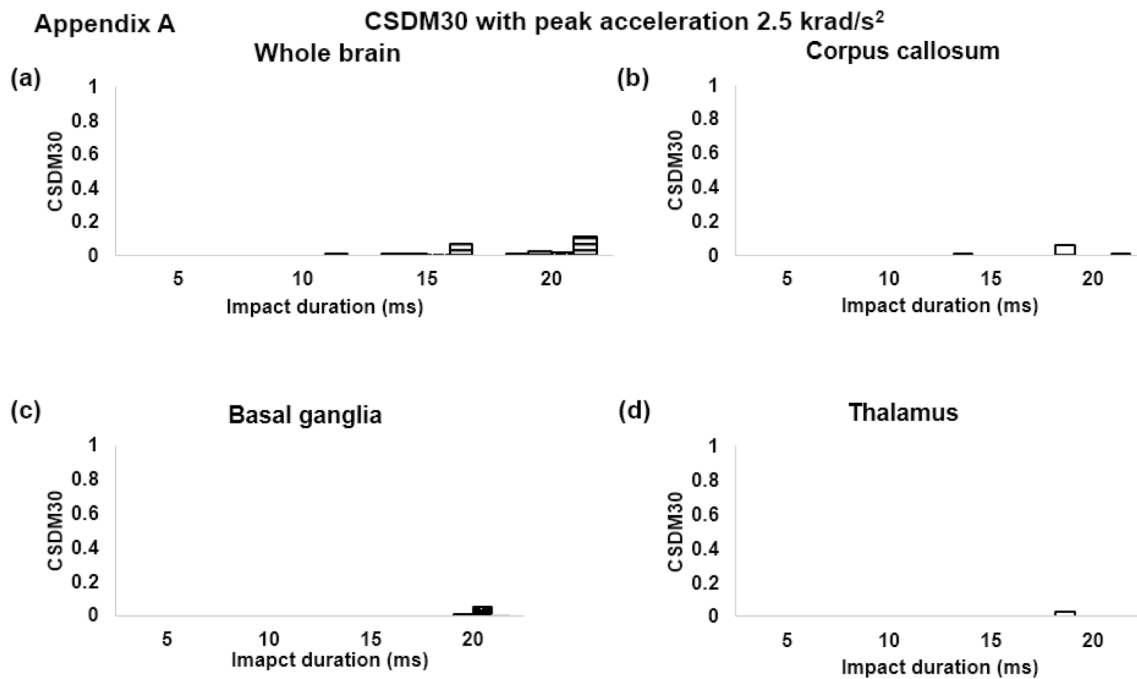
Results of CSDM25 for peak acceleration 2.5 krad/s².



Results of CSDM30 for peak acceleration 5 krad/s^2 .



Results of CSDM30 for peak acceleration 2.5 krad/s^2 .

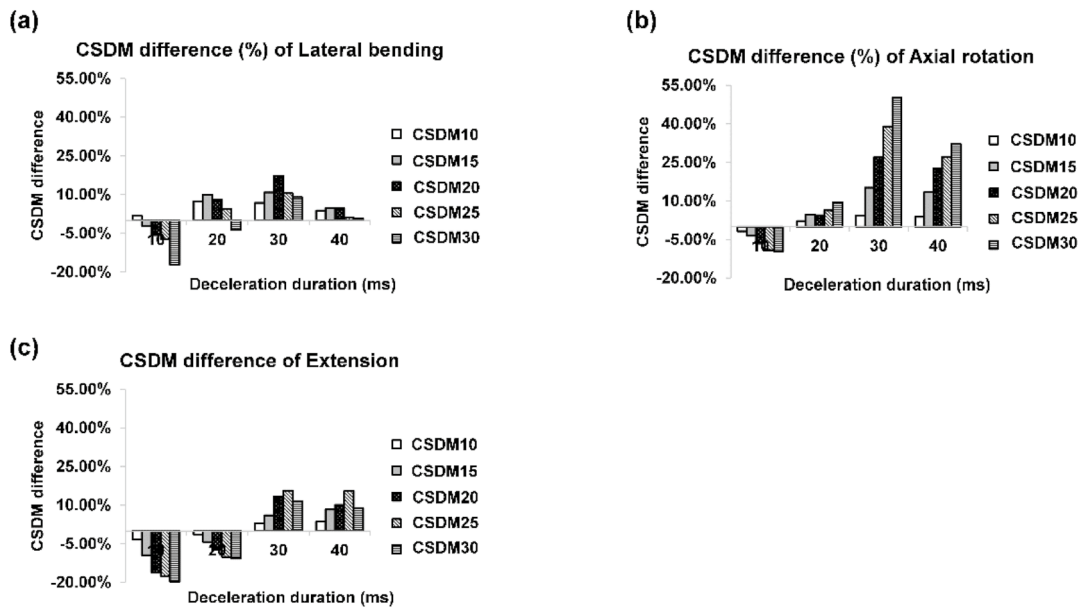


Appendix B: The effects of deceleration

CSDM difference of deceleration under lateral bending, lateral rotation and extension.

Appendix B

The effects of deceleration

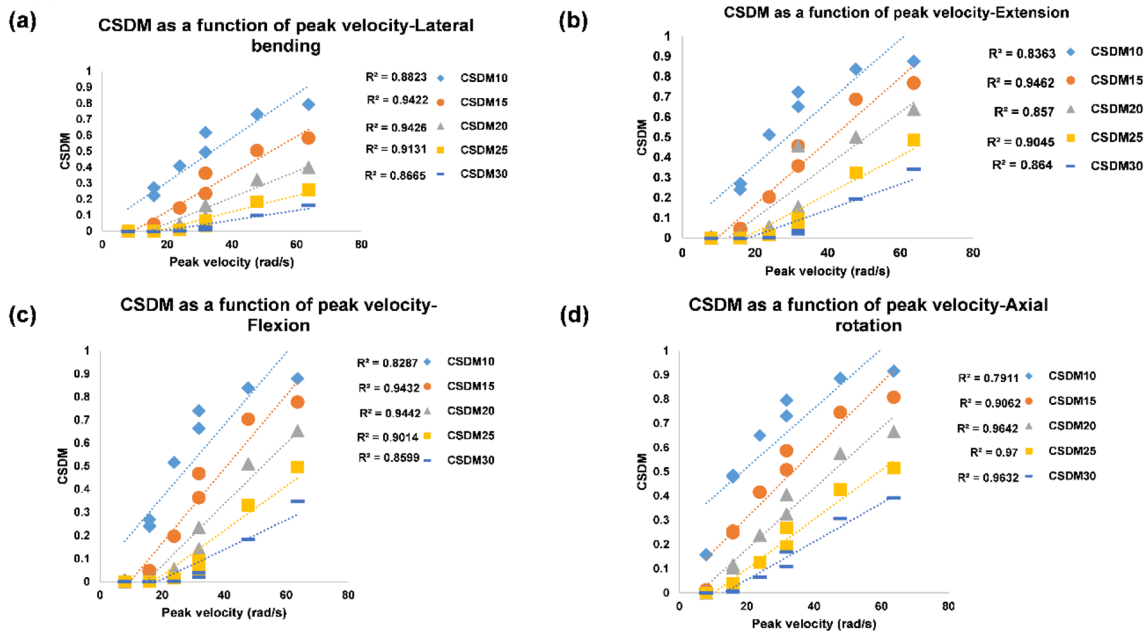


Appendix C: CSDM as a function of peak velocity under sine curve

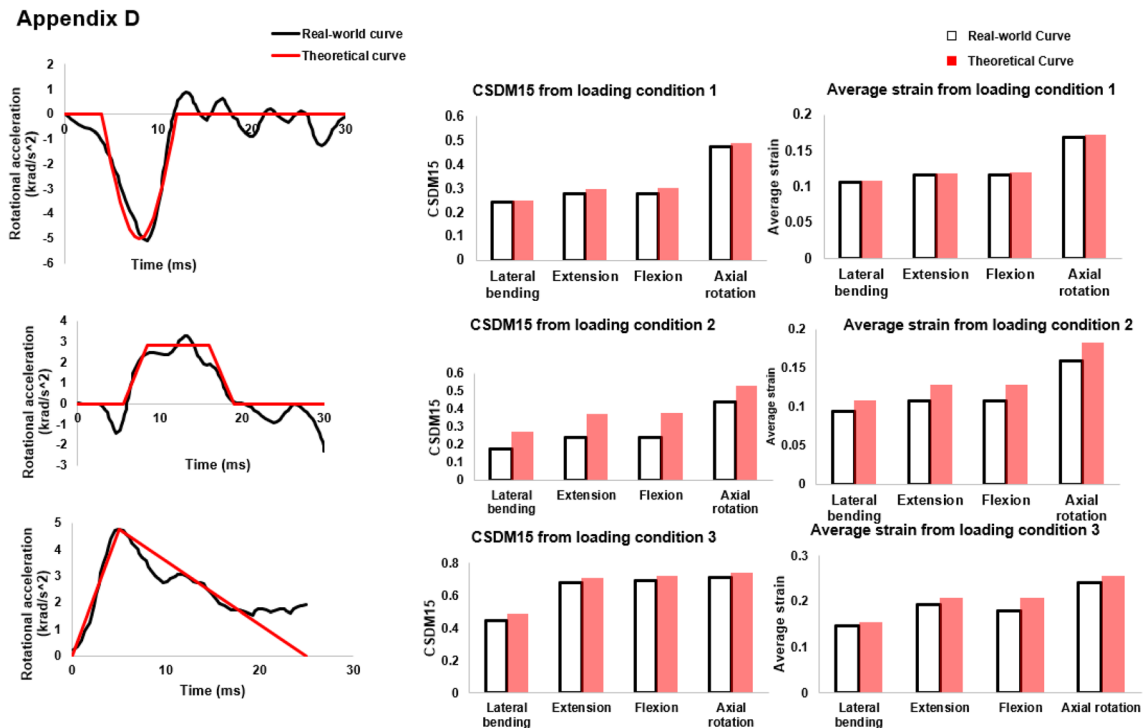
CSDM as a function of peak rotational velocity.

Appendix C

CSDM as a function of peak rotational velocity under sine curve



Appendix D: Differences in brain strain prediction between a real-world loading curve and a simplified theoretical curve



References

- Bain AC, Meaney DF (2000) Tissue-level thresholds for axonal damage in an experimental model of central nervous system white matter injury. *J Biomech Eng* 122:615–622
- Beckwith JG et al (2013) Timing of concussion diagnosis is related to head impact exposure prior to injury. *Med Sci Sports Exerc* 45:747–754. <https://doi.org/10.1249/MSS.0b013e3182793067>
- Chamard E, Lefebvre G, Lassonde M, Theoret H (2016) Long-term abnormalities in the corpus callosum of female concussed athletes. *J Neurotrauma* 33:1220–1226
- Elkin BS, Elliott JM, Siegmund GP (2016) Whiplash injury or concussion? A possible biomechanical explanation for concussion symptoms in some individuals following a rear-end collision. *J Orthop Sports Phys Ther* 46:874–885
- Elkin BS, Gabler LF, Panzer MB, Siegmund GP (2018) Brain tissue strains vary with head impact location: a possible explanation for increased concussion risk in struck versus striking football players. *Clin Biomech* 64:49–57
- Gabler LF, Joodaki H, Crandall JR, Panzer MB (2018) Development of a single-degree-of-freedom mechanical model for predicting strain-based brain injury responses. *J Biomech Eng* 140:031002
- Gadd CW (1966) Use of a weighted-impulse criterion for estimating injury hazard. In: SAE technical paper
- Graybiel AM (2000) The basal ganglia. *Curr Biol* 10:R509–R511
- Greenwald RM, Gwin JT, Chu JJ, Crisco JJ (2008) Head impact severity measures for evaluating mild traumatic brain injury risk exposure. *Neurosurgery* 62:789–798. <https://doi.org/10.1227/01.neu.0000311244.05104.96>
- Grossman EJ, Inglese M (2016) The role of thalamic damage in mild traumatic brain injury. *J Neurotrauma* 33:163–167
- Guskiewicz KM et al (2007) Recurrent concussion and risk of depression in retired professional football players. *Med Sci Sports Exerc* 39:903
- Guskiewicz KM, Mihalik JP (2011) Biomechanics of sport concussion: quest for the elusive injury threshold. *Exerc Sport Sci Rev* 39:4–11. <https://doi.org/10.1097/JES.0b013e318201f53e>
- Hardy WN, Foster CD, Mason MJ, Yang KH, King AI, Tashman S (2001) Investigation of head injury mechanisms using neutral density technology and high-speed biplanar X-ray. *Stapp Car Crash J* 45:337–368
- Hardy WN et al (2007) A study of the response of the human cadaver head to impact. *Stapp Car Crash J* 51:17
- Hernandez F et al (2019) Lateral impacts correlate with falx cerebri displacement and corpus callosum trauma in sports-related concussions. *Biomech Model Mechanobiol* 18(3):631–649
- Hoshizaki TB et al (2017) The development of a threshold curve for the understanding of concussion in sport. *Trauma* 19:196–206
- Kimpara H, Iwamoto M (2012) Mild traumatic brain injury predictors based on angular accelerations during impacts. *Ann Biomed Eng* 40:114–126
- King AI, Yang KH, Zhang L, Hardy W, Viano DC (2003) Is head injury caused by linear or angular acceleration. In: IRCOBI conference. Lisbon, pp 1–12
- Kleiven S (2005) Influence of direction and duration of impacts to the human head evaluated using the finite element method. In: International IRCOBI conference

- Kleiven S (2007) Predictors for traumatic brain injuries evaluated through accident reconstructions. *Stapp Car Crash J* 51:81–114
- Knowles BM, Dennison CR (2017) Predicting cumulative and maximum brain strain measures from hybridized head kinematics: a combined laboratory study and post-hoc regression analysis. *Ann Biomed Eng* 45:2146–2158
- Krave U, Al-Olama M, Hansson H-A (2011) Rotational acceleration closed head flexion trauma generates more extensive diffuse brain injury than extension trauma. *J Neurotrauma* 28:57–70
- Langlois JA, Rutland-Brown W, Wald MM (2006) The epidemiology and impact of traumatic brain injury: a brief overview. *J Head Trauma Rehabil* 21:375–378. <https://doi.org/10.1097/00001199-200609000-00001>
- Mao H et al (2013) Development of a finite element human head model partially validated with thirty five experimental cases. *J Biomech Eng* 135:111002
- Margulies SS, Thibault LE (1992) A proposed tolerance criterion for diffuse axonal injury in man. *J Biomech* 25:917–923. [https://doi.org/10.1016/0021-9290\(92\)90231-o](https://doi.org/10.1016/0021-9290(92)90231-o)
- McAllister TW, Ford JC, Ji S, Beckwith JG, Flashman LA, Paulsen K, Greenwald RM (2012) Maximum principal strain and strain rate associated with concussion diagnosis correlates with changes in corpus callosum white matter indices. *Ann Biomed Eng* 40:127–140
- McCrorry P, Meeuwisse W, Johnston K, Dvorak J, Aubry M, Molloy M, Cantu R (2009) Consensus statement on concussion in sport—the 3rd international conference on concussion in sport, held in Zurich, November 2008. *J Clin Neurosci* 16:755–763. <https://doi.org/10.1016/j.jocn.2009.02.002>
- Nahum AM, Smith R, Ward CC (1977) Intracranial pressure dynamics during head impact. In: SAE technical paper
- Newman J et al (1999) A new biomechanical assessment of mild traumatic brain injury. Part 1: Methodology. In: Proceedings of the international research conference on the biomechanics of impacts (IRCOBI), pp 17–36
- Patton DA, McIntosh AS, Kleiven S (2013) The biomechanical determinants of concussion: finite element simulations to investigate brain tissue deformations during sporting impacts to the unprotected head. *J Appl Biomech* 29:721–730
- Pellman EJ, Viano DC, Tucker AM, Casson IR (2003a) Concussion in professional football: Location and direction of helmet impacts—Part 2. *Neurosurgery* 53:1328–1341
- Pellman EJ, Viano DC, Tucker AM, Casson IR, Waeckerle JF (2003b) Concussion in professional football: reconstruction of game impacts and injuries. *Neurosurgery* 53:799–812
- Post A, Hoshizaki B, Gilchrist MD (2012) Finite element analysis of the effect of loading curve shape on brain injury predictors. *J Biomech* 45:679–683. <https://doi.org/10.1016/j.jbiomech.2011.12.005>
- Post A, Hoshizaki TB, Gilchrist MD, Cusimano MD (2017) Peak linear and rotational acceleration magnitude and duration effects on maximum principal strain in the corpus callosum for sport impacts. *J Biomech* 61:183–192
- Post A, Oeur A, Walsh E, Hoshizaki B, Gilchrist MD (2014) A centric/non-centric impact protocol and finite element model methodology for the evaluation of American football helmets to evaluate risk of concussion. *Comput Methods Biomed Eng* 17:1785–1800
- Rowson S, Brolinson G, Goforth M, Dietter D, Duma S (2009) Linear and angular head acceleration measurements in collegiate football. *J Biomech Eng Trans ASME* 131:7. <https://doi.org/10.1115/1.3130454>
- Rowson S et al (2012) Rotational head kinematics in football impacts: an injury risk function for concussion. *Ann Biomed Eng* 40:1–13. <https://doi.org/10.1007/s10439-011-0392-4>
- Rush GA, Rush GA, Sbravati N, Prabhu R, Williams LN, DuBien JL, Horstemeyer M (2017) Comparison of shell-facemask responses in American football helmets during NOCSAE drop tests. *Sports Eng* 20:199–211
- Sanchez EJ, Gabler LF, Good AB, Funk JR, Crandall JR, Panzer MB (2018) A reanalysis of football impact reconstructions for head kinematics and finite element modeling. *Clin Biomech* 64:82–89. <https://doi.org/10.1016/j.clinbiomech.2018.02.019>
- Shreiber DI, Bain AC, Meaney DF (1997) In vivo thresholds for mechanical injury to the blood-brain barrier. In: SAE technical paper
- Takhounts EG, Craig MJ, Moorhouse K, McFadden J, Hasija V (2013) Development of brain injury criteria (Br IC). *Stapp Car Crash J* 57:243
- Takhounts EG, Eppinger RH, Campbell JQ, Tannous RE (2003) On the development of the SIMon finite element head model. *Stapp Car Crash J* 47:107
- Takhounts EG et al. (2008) Investigation of traumatic brain injuries using the next generation of simulated injury monitor (SIMon) finite element head model. In: SAE technical paper
- Tang L, Ge Y, Sodickson DK, Miles L, Zhou Y, Reaume J, Grossman RI (2011) Thalamic resting-state functional networks: disruption in patients with mild traumatic brain injury. *Radiology* 260:831–840
- Thibault LE, Gennarelli TA, Margulies SS, Marcus J, Eppinger R (1990) The strain dependent pathophysiological consequences of inertial loading on central nervous system tissue. In: International conference on the biomechanics of impacts, Bronx
- Trosseille X, Tarriere C, Lavaste F, Guillon F, Domont A (1992) Development of a FEM of the human head according to a specific test protocol. In: SAE technical paper
- Versace J (1971) A review of the severity index. In: SAE technical paper
- Viano DC, Casson IR, Pellman EJ, Zhang L, King AI, Yang KH (2005) Concussion in professional football: brain responses by finite element analysis: part 9. *Neurosurgery* 57:891–916
- Viano DC, Lovsund P (1999) Biomechanics of brain and spinal-cord injury: analysis of neuropathologic and neurophysiology experiments. *Traffic Injury Prev* 1:35–43
- Yoganandan N, Li J, Zhang J, Pintar FA, Gennarelli TA (2008) Influence of angular acceleration–deceleration pulse shapes on regional brain strains. *J Biomech* 41:2253–2262
- Zhang L, Yang KH, King AI (2001) Comparison of brain responses between frontal and lateral impacts by finite element modeling. *J Neurotrauma* 18:21–30
- Zhang L, Yang KH, King AI (2004) A proposed injury threshold for mild traumatic brain injury. *J Biomech Eng* 126:226–236
- Zhao W, Ji S (2017) Brain strain uncertainty due to shape variation in and simplification of head angular velocity profiles. *Biomech Model Mechanobiol* 16:449–461

Publisher's Note Springer Nature remains neutral with regard to jurisdictional claims in published maps and institutional affiliations.